frontiers | Frontiers in Energy Research

TYPE Original Research
PUBLISHED 23 October 2023
DOI 10.3389/fenrg.2023.1247153

OPEN ACCESS

EDITED BY
Karunesh Kant,
Virginia Tech, United States

REVIEWED BY
Sunil K. Sansaniwal,
Malaviya National Institute of Technology, Jaipur, India
Xingan Liu,
Shenyang Agricultural University, China

*CORRESPONDENCE
Shimao Cui,
cuishimao@sina.com

†These authors have contributed equally to this work and share first authorship

RECEIVED 25 June 2023
ACCEPTED 10 October 2023
PUBLISHED 23 October 2023

CITATION
Sun Q, Song Y, Yang Z, Liu X and Cui S (2023), Analysis of the light performance of Chinese solar greenhouse with internal insulation based on a solar radiation model.
Front. Energy Res. 11:1247153.
doi: 10.3389/fenrg.2023.1247153

Analysis of the light performance of Chinese solar greenhouse with internal insulation based on a solar radiation model

Qian Sun[1†], Yang Song[1†], Zhigang Yang[2], Xiaorui Liu[2] and Shimao Cui[1*]

[1]College of Horticulture and Plant Protection, Inner Mongolia Agricultural University, Hohhot, China, [2]Institute of Vegetables and Flowers, Inner Mongolia Academy of Agricultural and Animal Husbandry Sciences, Hohhot, China

Chinese solar greenhouses are important agricultural building facilities with highly efficient and sustainable solar energy consumption. A solar greenhouse with an external insulation blanket for heat preservation is the most prevalent type of CSG. However, greenhouse performance degrades as the thermal insulation performance of the external blanket deteriorates over time when the blanket is exposed to harsh environmental conditions. Moreover, the external blanket is usually parked in an inconvenient location on the south roof in the practice, resulting in shading owing to its increasing coverage length. This significantly influences the solar radiation received by the south roof and that projected on the wall, ultimately affecting the light performance of the greenhouse. Therefore, a solar greenhouse with an innovatively applied internal insulation system was proposed in this study. To analyze the light performance of the solar greenhouse, a solar radiation model was established and verified by comparing the measured and calculated values. Based on the calculated model results, the spatial distribution of solar radiation inside the greenhouse and its allocation to the interior surfaces of the greenhouse were simulated. The total captured and transmitted solar radiation accumulations were compared for three different roof shapes. The captured and transmitted radiation accumulation of the greenhouse with internal insulation increased by 3.9–9.5 and 1.8–4.4 MJ compared to the two other greenhouses, respectively. The effect of the position of the parked blanket on the beam solar radiation projected on the wall and ground was considered. The results indicated that the increased blanket coverage length decreased the cumulative radiation on the wall by 25.24%–99.82%, which did not contribute to improving greenhouse energy-saving production. This study provides a new approach to greenhouse design and optimization.

KEYWORDS

Chinese solar greenhouses, solar energy utilization, internal insulation, solar radiation model, light performance, greenhouse optimization

1 Introduction

Greenhouse production is the most important component of agriculture and contributes significantly to agricultural efficiency. In greenhouses, an appropriate microclimate is created for plant growth, isolated from external natural conditions, rendering fresh fruits and vegetables available in all seasons (Bazgaou et al., 2020a). Therefore, greenhouse cultivation can achieve higher yield and quality than open-field farming (Bazgaou et al., 2020b; Esmaeli and Roshandel, 2020). However, maintaining an optimal environment in a well-operated greenhouse requires energy to meet the heating, cooling, ventilation, and lighting demands (Cuce et al., 2016; Hassanien et al., 2016; Trypanagnostopoulos et al., 2017; Aldaftari et al., 2019). With the development of scale and industrialization in modern agricultural facilities, greenhouse energy systems are still met by burning large amounts of fossil fuels, contributing to greenhouse gas emissions and damaging the environment (Vadiee and Martin, 2012; Taki et al., 2018; Chen et al., 2020). The constant increase in fossil fuel prices has also significantly intensified greenhouse production costs (Canakci et al., 2013; Shukla et al., 2016).

As fossil energy increasingly depletes and the environmental pollution caused by fossil fuel combustion worsens, energy selection and utilization in agricultural greenhouses have become critical issues. Therefore, the development of sustainable agriculture requires alternative renewable energy sources and energy-saving solutions (Cuce et al., 2016; Gorjian et al., 2021). In recent decades, renewable energy sources such as ground or air source heat pumps (Lund et al., 2005), photovoltaic/thermal systems (Cossu et al., 2014) and biomass energy (Bibbiani et al., 2017) have been widely applied in agricultural greenhouses to reduce energy consumption. Solar energy is considered the foremost greenhouse energy source due to its sustainability, cleanliness, affordability, safety, and abundance; it effortlessly provides ample illumination and thermal energy. The utilization of solar energy in greenhouses effectively meets their energy requirements. The transparent enclosure of solar greenhouses facilitates the entry of solar energy into their interiors, thereby influencing the formation and development of the light environment. Solar greenhouses are meticulously designed to maximize solar energy acquisition. To optimize the performance of greenhouse solar energy utilization, various factors that significantly impact the amount of received solar radiation have been extensively investigated, including greenhouse building design parameters and implementation of advanced energy-harvesting technologies (Raptis et al., 2017). Bot et al. (2005) designed a solar greenhouse system that required less energy and achieved energy savings of over 60% by capturing solar energy during summer months and storing it in an underground aquifer at moderate temperatures. The stored energy is subsequently used during the winter months using heat pumps. Sethi (2009) proposed a mathematical model to compute transmitted solar radiation for selected geometry greenhouses to identify the best greenhouse type and orientation. Singh and Tiwari (2010) identified the optimum greenhouse by evaluating the highest available solar energy and lowest additional energy requirement. Çakır and Şahin (2015) computed the seasonal total solar energy gain rate for five greenhouse types to reveal that an elliptical greenhouse was the optimum greenhouse for use in cold climate regions in Turkey. El-Maghlany et al. (2015) provided an analytical solution to calculate the amount of captured solar energy for elliptically curved surfaces with different aspect ratios and found that the solar energy capture reached a maximum value at an aspect ratio of 4. Tang et al. (2020) investigated the effectiveness of a solar greenhouse that utilized opaque photovoltaic (OPV) modules and a solar-combined air-source heat pump system. The results showed that the indoor temperature was 5.3°C–7.3°C higher than the ambient temperature during the coldest period in Kunming City when using the heating system. The optimization of greenhouse structures and the utilization of solar energy technologies in solar greenhouses enhance the implementation of energy-saving strategies. However, exploring methods to minimize energy consumption and improve energy utilization efficiency in greenhouses remains a significant challenge.

In China, as an unique type of solar energy collectors, Chinese solar greenhouses (CSGs) are widely promoted in China owing to their energy savings, improved efficiency, reduced energy consumption, and low costs. Most CSGs in China are located north of the Yangtze River, including in northern, northeastern, and northwestern China, and have developed rapidly in these regions. CSGs provide high-quantity and high-quality agricultural products, thereby increasing farmers' incomes. Although CSGs frequently encounter harsh environmental conditions in cold winters, they have achieved notable economic and social benefits (Tong et al., 2022). CSGs allow shortwave solar radiation to be transmitted through the transparent south roof covered with plastic film to strike the internal opaque surface, where part of the solar energy is provided for plant photosynthesis, and the rest is reflected out of the greenhouses or converted to heat that can be absorbed and stored by the wall and ground. Due to the discontinuous solar energy supply at night, thermal blankets are generally used to cover the southern roof to prevent heat loss and improve indoor thermal comfort. Meanwhile, the temperature difference between the interior and exterior forces the northern wall and ground to release stored heat as an energy supplement for the thermal losses of the internal air temperature dropping (Li et al., 2010; Liu et al., 2022). In addition, because the north roof is generally made of lightweight thermal insulation materials, it plays a significant role in retaining absorbed solar energy indoors. The aforementioned building structures enveloping the enclosure space represent a typical CSG.

In comparison to other greenhouse types worldwide, CSGs demonstrate consistent operation with minimal or no additional heating, particularly in cold regions of China under adverse weather conditions. A comfortable indoor environment, which directly influences plant physiological processes, is provided by CSGs. The solar radiation transmitted through the transparent roof enters the greenhouse interior forming a light environment that depend on the transmittance and the distribution of solar radiation. The solar radiation received by the crop canopy facilitates photosynthesis, while the solar radiation projected onto interior

surfaces of CSGs, such as the ground and north wall, is absorbed and stored as heat, and released to enhance the thermal environment. Therefore, the rational design of structures plays a crucial role in maximizing the interception of solar energy by CSGs. This the reason that the south roof was designed to obtain more energy from the sun. Moreover, in CSGs, the thermal environment directly benefits from the heat storage facilitated by the north wall. Approximately 1/3 of the solar radiation on the transparent south roof reaches the north wall surface and increases the temperature, increasing the indoor air temperature by up to 10°C (Wei et al., 2016; Zhang et al., 2016). This means that the light performance of a solar greenhouse directly determines its heat gain, thereby affecting energy savings in the greenhouse.

Numerous studies have evaluated the light environment in greenhouses by analyzing the influencing factors. Tong et al. (2018) studied solar heat gains in greenhouses with different spans using computational fluid dynamics (CFD). A large span received sufficiently more solar energy, whereas the tested CSGs had the same north roof and north wall dimensions. Xu et al. (2020) used a solar radiation model to study the effects of orientation and structure on solar radiation interception in CSGs. Optimizing the structural ridge height and horizontal projection of the rear roof improved the solar energy interception of CSG-LS. Chen et al. (2018) proposed a method for solar greenhouses to determine the optimal orientation to maximize solar energy collection by the south roof. Wang et al. (2010) simulated the sunlight transmitted through four different curvilinear roofs of a solar greenhouse. The greenhouse with a three-spline roof exhibited more sunlight permeation than those with the other roofs. Zhang et al. (2014) found that lighting performance was rarely improved by changing the shape of the south roof; they designed a tilting-roof solar greenhouse using active daylighting technology under these circumstances. The study showed that the dip angle of the tilted roof was actively adjusted based on solar altitude, and the daylighting performance increased by 25.05% compared to the fixed-roof solar greenhouse.

In addition, simulated models have been widely recognized and applied to evaluate the lighting performance and optimize the structural design of solar greenhouses. Tong and Li (2006) proposed a mathematical model to simulate solar radiation on solar greenhouse surfaces. An inclined plane was used instead of a curved surface to analyze the influence of greenhouse-building parameters. The results showed that the changes in span and height affected solar radiation on the ground and north wall. Han et al. (2014) calculated the direct, diffuse, and total solar radiation at any point inside a greenhouse on clear days using a model that considered the prevailing view angle. Ma et al. (2013) established a light environment model for solar greenhouses that reflected many factors to determine the relationship between the calculated point and the incident solar radiation. Xu et al. (2019) established a comparatively perfect solar radiation model to analyze the internal radiation changes in greenhouses. This model, based on summarizing previous models, considers the relationship between the sun's rays and the angle of the front roof. Zhang et al. (2020) developed a mathematical model for solar greenhouses to evaluate the light environment quantitatively. The model was used to obtain the spatial distribution of solar radiation by considering the evolution of interior solar radiation in a solar greenhouse. Huang et al. (2020) proposed an analytical model to evaluate the total solar radiation transmitted to the curved surface of a solar greenhouse. The simulated results showed that the equivalent beam transmissivity could be accurately calculated using an actual curved surface instead of traditional simplified inclined planes. These models describe the solar radiation received by the solar greenhouses. However, the solar greenhouses used in these models are typical, with a fixed transparent film covering the south roof and an external thermal blanket that can be rolled up. In production practice, the external thermal blankets frequently directly encounter harsh natural environmental conditions and are affected by many factors, such as rain, snow, and frost. This situation results in a decline in thermal performance and an increase in greenhouse management and production costs, thereby minimizing profitability and sustainability. Currently, no material simultaneously exhibits low weight, aging resistance, water resistance, tear resistance, peel resistance, and low thermal conductivity. Although the thermal blanket of composite materials demonstrates a better thermal insulation effect, its weight and cost increase with the number of materials used. Such blankets of composite materials could not sustainably resist the effects of the harsh environment of high altitude and cold regions. In addition, thermal blankets negatively affect the solar radiation transmitted into the greenhouse and the solar energy projected on the north wall, as thermal blankets often stop at an inappropriate position on the south roof, leading to shading caused by the increasing coverage length of the blanket (Tong et al., 2010; Zhang et al., 2020).

Because of the complex and diverse climate conditions in different regions of China, selecting a suitable type of solar greenhouse is crucial to ensure optimum light and thermal performance based on the local environment. Inner Mongolia in northern China is located in the middle and high latitudes (Wu et al., 2023). Because of its sufficient solar radiation, Inner Mongolia is ideal for developing a solar greenhouse industry. However, thermal blankets are easily affected by severe environmental conditions during harsh winters. To mitigate the impact of harsh environmental conditions on the performance of thermal blankets, it is imperative to implement an internal insulation system within solar greenhouse interiors, thereby enhancing the insulation efficiency of greenhouses. Hence, a passive solar greenhouse with internal insulation comprising an interior thermal blanket on an independent steel frame in the greenhouse, as shown in Figure 1, was designed and built for crop cultivation in high latitudes and cold regions. Similar to the air-inflated double-plastic covered greenhouse, a solar greenhouse with an interior blanket, as opposed to a typical solar greenhouse with an external thermal blanket, develops an effective internal thermal insulation space when the blanket is closed at sunset. The interior thermal blanket is thinner and more durable than the external thermal blanket at the same thermal resistance level. The north roof of the greenhouses with internal insulation is also transparent as the south roof because both comprise an entire plastic film. The light performance of a solar greenhouse directly determines how well a greenhouse system operates. It creates comfortable light conditions for crop photosynthesis and ensures adequate solar energy storage by the north wall, which is generally beneficial for the thermal environment.

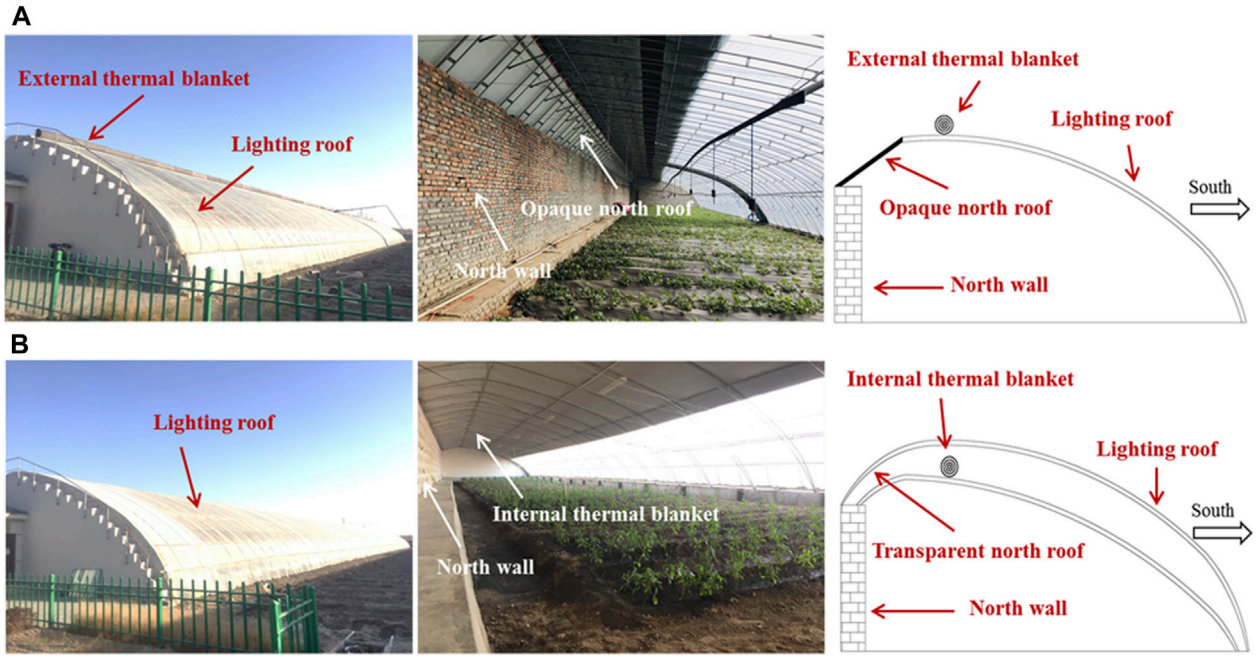

FIGURE 1
Photographic and schematic diagrams of **(A)** a Chinese solar greenhouse with an external thermal blanket and **(B)** a Chinese solar greenhouse with an internal thermal blanket.

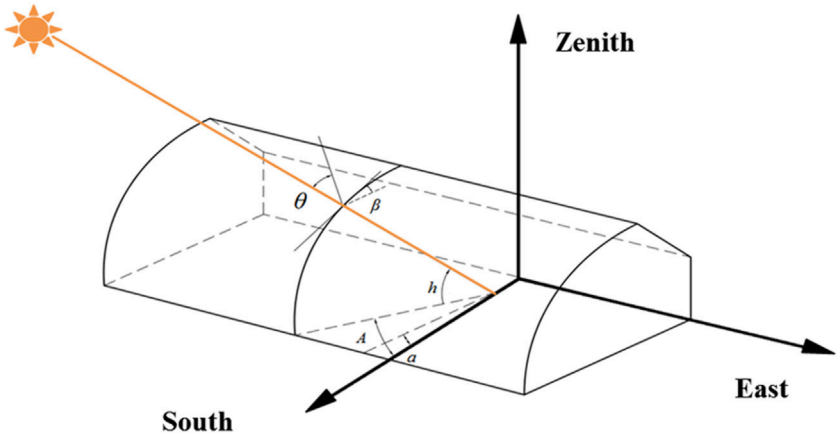

FIGURE 2
Schematic diagram of the spatial relationship between the sun and the solar greenhouse.

In this study, a solar radiation model was established and used to evaluate the light environment performance of a solar greenhouse with internal insulation, including the solar energy captured by the roof and the solar radiation distribution transmitted into the greenhouse. The model accuracy was verified by comparing its simulation results with the field measurement results. The model provided new insights and theoretical guidance for the optimal design of greenhouse structures and the selection of greenhouse types to reduce production costs and improve the light and thermal performance of solar greenhouses in northern China.

2 Materials and methods

2.1 Mathematical model

2.1.1 Spatial relationship of the sun and the solar greenhouse

The maximum received solar radiation for a solar greenhouse depends on the relative position between the sun and the solar greenhouse. When designing a solar greenhouse in certain regions at certain geographical latitudes, the dynamic changes in the sun must be considered. Solar radiation projected onto an inclined plane

changes with the sun's position throughout the day. Furthermore, the received solar radiation from a solar greenhouse varies with the position of the curved roof. Figure 2 shows the spatial relationship between the sun and the solar greenhouse. Beam solar radiation represents the main direction of solar rays, and another scattered solar radiation has the characteristic of isotropy, overlooking the direction. The equations for the related angles are as follows:

$$\theta_{(t)} = \cos^{-1}\left(\cos\beta \times \sin h_{(t)} + \sin\beta \times \cos h_{(t)} \times \cos\left(A_{(t)} - a\right)\right) \quad (1)$$

In Eq. 1, θ is the incident angle of the beam solar radiation on the curved roof, and the slope angle β of the solar radiation incident point on the roof varies along the roof. h is the solar altitude angle, A is the solar azimuth angle, and a is the solar greenhouse azimuth angle. Subscript t indicates that the corresponding angles vary dynamically with time. h and A were calculated as follows:

$$h_{(t)} = \sin^{-1}\left(\sin\varphi_{LOCAL} \times \sin\delta + \cos\varphi_{LOCAL} \times \cos\delta \times \cos\omega_{(t)}\right) \quad (2)$$

$$A_{(t)} = \sin^{-1}\left(\frac{\cos\delta \times \sin\omega_{(t)}}{\cos h_{(t)}}\right) \quad (3)$$

where ϕ_{LOCAL}, δ, and ω refer to the geographical latitude of the solar greenhouse, the solar declination angle, and the hour angle, respectively. δ and ω were calculated as follows:

$$\delta = 23.45 \times \sin\left(\frac{360 \times (284 + DN)}{365}\right) \quad (4)$$

$$\omega_{(t)} = 15 \times (T_{LOCAL} - 12) \quad (5)$$

$$T_{LOCAL} = T_{STANDARD} + \frac{\gamma_{LOCAL} - \gamma_{STANDARD}}{15} + \frac{ET}{60} \quad (6)$$

$$ET = 9.87 \times \sin 2B - 7.53 \times \cos B - 1.5 \times \sin B \quad (7)$$

$$B = \frac{360 \times (DN - 81)}{364} \quad (8)$$

where DN represents the number of days. T_{LOCAL} and $T_{STANDARD}$ refer to the local apparent solar time and Beijing time, respectively. γ_{LOCAL} and $\gamma_{STANDARD}$ refer to the local longitude and standard longitude of Beijing time, respectively. ET is the time difference between the local position and Beijing time.

2.1.2 Solar radiation captured and transmitted by the solar greenhouse roof

When solar radiation reaches the curved roof of a solar greenhouse in a day, the daily cumulative solar radiation Q_{cap} captured by the external surface of the greenhouse roof is expressed using Eq. 9.

$$Q_{cap} = \int_{T_{sr}}^{T_{ss}} \int_{0}^{L_{roof}} I_{cap} dL dT \quad (9)$$

Generally, the solar radiation on Earth includes beam and diffuse solar radiation. In Eq. 9, T_{ss} and T_{sr} refer to the times of sunset and sunrise on the roof, respectively. L_{roof} denotes the roof length. The captured solar radiation intensity I_{cap} of the external surface was calculated as follows:

$$I_{cap} = I_{b(t),roof} + I_{d(t),roof} \quad (10)$$

$$I_{b(t),roof} = I_0 \times \cos\theta_{(t)} \times P^M \quad (11)$$

$$I_{d(t),roof} = \frac{I_0 \times \sin h_{(t)} \times \cos^2\frac{\beta}{2} \times \left(1 - P^M\right)}{2 - 2.8 \times \ln P} \quad (12)$$

where $I_{b(t),roof}$ and $I_{d(t),roof}$ refer to the solar beam radiation intensity and diffuse radiation intensity on the roof with a slope angle β, respectively. I_0 is extraterrestrial solar radiation, P is the atmospheric transparency coefficient, and M is atmospheric mass. I_0 and M were calculated using Eqs. 13,14, respectively.

$$I_0 = 1367 \times \left(1 + 0.034 \times \cos\frac{360 \times DN}{365}\right) \quad (13)$$

$$M = \begin{cases} \dfrac{1}{\sin h_{(t)}}, \left(h_{(t)} > 30^\circ\right) \\ \left(1229 + \left(614 \times \sin h_{(t)}\right)^2\right)^{0.5} - 614 \times \sin h_{(t)}, \left(h_{(t)} \le 30^\circ\right) \end{cases} \quad (14)$$

When the thermal blanket was rolled up, the solar radiation entered the solar greenhouse through a transparent film covering the roof. The daily cumulative transmitted solar radiation Q_{trans} through the greenhouse roof is expressed using Eq. 15.

$$Q_{trans} = \int_{T_{op}}^{T_{cl}} \int_{0}^{L_{roof}} I_{trans} dL dT \quad (15)$$

where T_{op} and T_{cl} are the opening and closing times of the thermal blanket, respectively, which influence the lighting time of the solar greenhouse. The amount of solar energy transmitted to the solar greenhouse is strongly influenced by the transmittance of the transparent film. Hence, the transmitted solar radiation intensity I_{trans} through the transparent roof was expressed as follows:

$$I_{cap} = I_{b(t),trans} + I_{d(t),trans} \quad (16)$$

$$I_{b(t),trans} = \tau_{b(t),\theta} \times I_{b(t),roof} \quad (17)$$

$$I_{d(t),trans} = \tau_d \times I_{d(t),roof} \quad (18)$$

where $I_{b(t),trans}$ and $I_{d(t),trans}$ refer to the transmitted solar beam radiation intensity and the transmitted solar diffuse radiation intensity of the internal solar greenhouse, respectively. $\tau_{b(t),\theta}$ represents the solar beam radiation transmittance, which varies with the solar position and sola radiation incident angle θ. τ_d is the solar diffuse radiation transmittance. $\tau_{b(t),\theta}$ and τ_d were calculated using Eqs. 19, 20, respectively.

$$\tau_{b(t),\theta} = \tau_{b(t),\theta} \times \left(1 - 0.93^{(90-\theta)}\right) \times \left(1 - \frac{\theta}{1000}\right) \quad (19)$$

$$\tau_d = \tau_{d0} \times (1 - \sigma_1) \times (1 - \sigma_2) \times (1 - \sigma_3) \quad (20)$$

where τ_{b0} is the beam radiation transmittance of the clear transparent film at an incident angle of 0°, τ_{d0} is the diffuse radiation transmittance of the clear transparent film, and σ_1, σ_2, and σ_3 are the solar radiation transmission attenuations caused by some factors, including the surface cleanliness and aging of the transparent film and envelope shading, respectively (Ma et al., 2013).

2.1.3 Solar radiation distribution of the solar greenhouse interior

A CSG was designed and built as a passive solar energy collector to maximize solar radiation gain for utilizing luminous and thermal energy. When the transmitted solar radiation enters the solar greenhouse, it projects onto the internal surfaces of the greenhouse structure and crop leaves, providing photosynthetically active radiation required for crop photosynthesis and a suitable level of indoor air temperature for

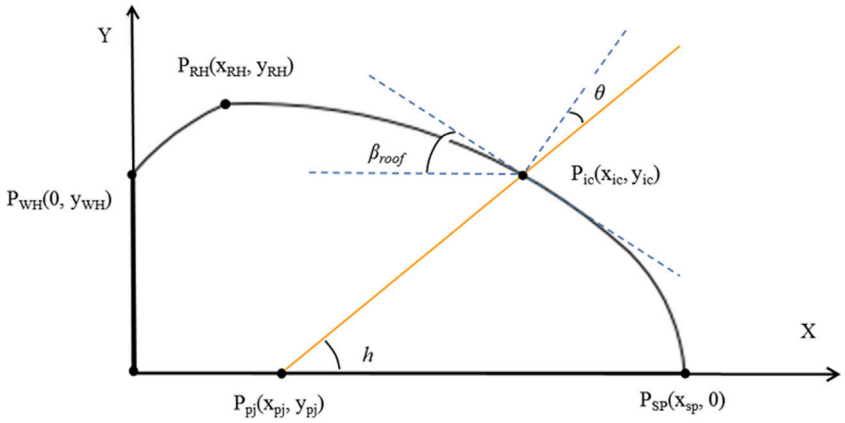

FIGURE 3
Cross-section diagram of sun rays projected in the solar greenhouse.

crop growth support. Additionally, internal solar radiation projected onto the ground and inner surface of the wall is collected and converted into thermal energy for storage and release during greenhouse operation. Subsequently, the solar radiation obtained from the solar greenhouse significantly contributes to forming the essential light and thermal environment. The specific solar radiation distribution inside a solar greenhouse will help guide optimization design theory and practical production based on energy savings.

An arbitrarily projected point of transmitted solar radiation in a greenhouse space has a sunray incident point on the curved roof. With the unconsidered beam radiation direction change affected by the thin transparent film, the beam radiation propagates through the incident point onto the projected point, representing the sunray propagation path. A coordinate system was established to reflect the physical relationship between the solar greenhouse structure and sunlight (Figure 3). In the coordinate system, the point of intersection of the north wall and horizontal ground is the origin of the coordinates, and the north wall point P_{WH}, ridge point P_{RH}, and span point P_{SP} are the three basic points of the roof curve. The curved roof was fitted, and its curve equation is expressed in Eq. 21.

$$\boldsymbol{y = F(x)} \tag{21}$$

In Eq. 21, the roof curve can be transformed into many forms, including parabolic, oval, circular, and double-section arc curves, which are commonly used in roofs.

The equation of the sunray path that transmits through point P_{ic} on the roof and projects point P_{pj} inside the greenhouse is given in Eq. 22.

$$\boldsymbol{y = \frac{tanh_{(t)}}{cos(A_{(t)} - a)} \times (x - x_{pj}) + y_{pj}} \tag{22}$$

where x_{pj} and y_{pj} represent the coordinate points of projected point P_{pj}.

When point P_{pj} is on the ground, the daily cumulative projected solar radiation $Q_{pj,g}$ on the ground can be expressed as:

$$\boldsymbol{Q_{pj,g} = \int_{T_{op}}^{T_{cl}} \int_{0}^{L_{span}} I_{pj,g} dL dT} \tag{23}$$

where $I_{pj,g}$ is the projected solar radiation intensity of point P_{pj} on the ground. L_{span} denotes the span length. I_{pj} can be expressed as follows (Zhang et al., 2020).

$$\boldsymbol{I_{pj,g} = I_{b(t),pj} \times I_{d(t),pj}} \tag{24}$$

$$\boldsymbol{I_{b(t),pj} = \frac{sin\left(tan^{-1}\left(\frac{tanh_{(t)}}{cos(A_{(t)} - a)}\right) + \beta\right)}{sin\left(tan^{-1}\left(\frac{tanh_{(t)}}{cos(A_{(t)} - a)}\right)\right)} \times I_{b(t),trans}} \tag{25}$$

$$\boldsymbol{I_{d(t),pj} = \frac{1}{L_{pj}} \times X_{roof,pj} \times \int_{0}^{L_{roof}} I_{d(t),trans} dL} \tag{26}$$

$$\boldsymbol{X_{roof,pj} = \frac{1}{L_{roof}} \times \int_{0}^{L_{roof}} \int_{0}^{L_{pj}} \frac{cos\,\varepsilon_{roof} \times cos\,\varepsilon_{pj}}{\pi S^2} dL_{roof} dL_{pj}} \tag{27}$$

where $X_{roof,pj}$ is the view factor from the roof to the projected surface, representing the fraction of the diffuse radiation leaving the roof intercepted by the projected surface in the two-dimensional greenhouse cross-section. S denotes the length of the connection line between the roof and the projected surface. ε_{roof} and ε_{pj} indicate the angles between the connection line and its normal, respectively.

2.2 Experimental conditions

A CSG with an internal thermal blanket (CSG-ITB) was used as the experimental subject. The measurement and simulation results were used to validate model accuracy. CSG-ITB is located in Hohhot, Inner Mongolia, China (40.8°N, 111.7°E), with its orientation facing south and a 5° movement from south to west. The east–west length of the CSG-ITB was 50 m. CSG-ITB had two independent steel frames. The upper frame was covered with a polyolefin film, in which both the south and north roofs were transparent, and a rolling thermal blanket was placed in the lower frame. The equivalent slope angle of the roof was 30°. The span, ridge height, and north wall height were 9, 4.3, and 3.2 m, respectively. To acquire an accurate distribution of the inner solar radiation, the CSG-ITB had no crops, and the opening and closing times of the thermal blanket were 9:00 and 16:00, according to general practice. The light transmittance of the clear PO film was

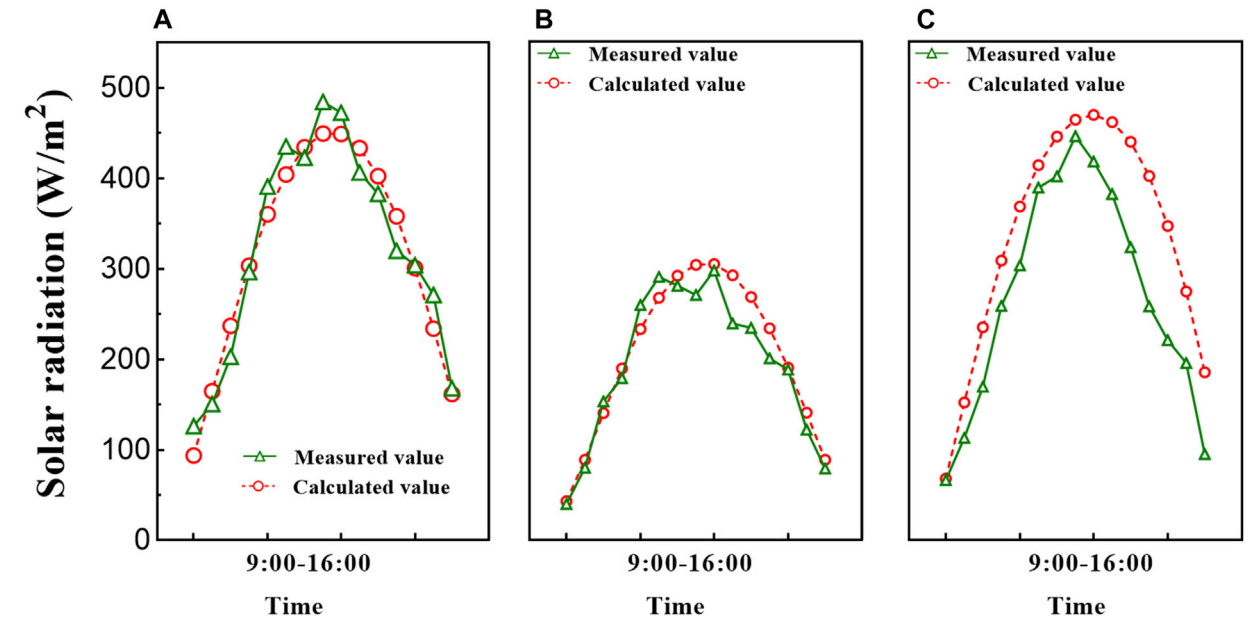

FIGURE 4
Comparison of calculated and measured values of solar radiation indoors and outdoors: **(A)** outdoor; **(B)** ground; **(C)** wall.

85%. The roof comprised three arcs, and the fitting curved equation for the roof in Eq. 21 can be expressed using Eq. 28. The slope angle β (Eq. 29) at each point on the roof was obtained by taking the derivative along the roof curved equation (Eq. 28). The outside and inside solar radiation were measured using PDE-KC recorders, with a measurement range of 0–2000 W/m^2 and an accuracy of 5%. The measurement points were located at the center of the greenhouse, which was placed 1.5 m above the ground. The outside measurement point was placed 1.5 m above open ground. The experiment was conducted from 1 December 2014 to 1 March 2015, and a typical sunny day (10 January 2015) was selected as a sample for model validation.

$$y = F(x) = \begin{cases} (17.72 - (x - 3.22)^2)^{0.5} + 0.44, (0 \le x < 1.5) \\ (141.13 - (x - 0.97)^2)^{0.5} - 7.57, (1.5 \le x < 8.1) \\ (8.76 - (x - 6.05)^2)^{0.5} - 0.2, (8.1 \le x \le 9) \end{cases} \tag{28}$$

$$\beta = \begin{cases} \tan^{-1}\left(\frac{x - 3.22}{y - 0.44}\right), (0 \le x < 1.5) \\ \tan^{-1}\left(\frac{x - 0.97}{y + 7.57}\right), (1.5 \le x < 8.1) \\ \tan^{-1}\left(\frac{x - 6.05}{y + 0.2}\right), (8.1 \le x \le 9) \end{cases} \tag{29}$$

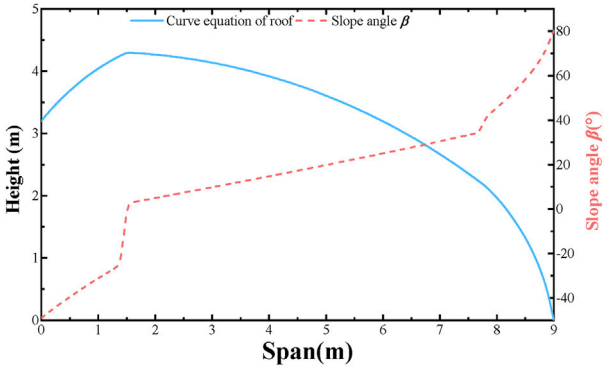

FIGURE 5
Curve equation and slope angle of the solar greenhouse roof.

3 Results and discussion

3.1 Model validation

To validate the accuracy of the established solar radiation model, solar radiation was measured in CSG-ITB from 9:00 to 16:00, which is the lighting time with the thermal blanket opening at 9:00 and closing at 16:00 on a typical sunny day (10 January 2015). The solar radiation intensity values from the measurement and simulation results at different positions were compared (Figure 4). The measured and calculated values adequately matched the overall variation trend (Figure 4). Outdoors, the mean absolute error (MBA) and the root mean square error (RMSE) were 23.48 and 26.23 W/m^2, respectively. Inside the solar greenhouse on the ground, the MBA and RMSE were 29.69 and 38.48 W/m^2, respectively. On the north wall of solar greenhouse, the MBA and RMSE were 66.31 and 77.83 W/m^2, respectively. The coefficient of determination (R^2) was 0.89–0.96, indicating model reliability. However, the measured values for the wall were consistently lower than the calculated values, as the position of the internal thermal blanket probably caused a decline in solar

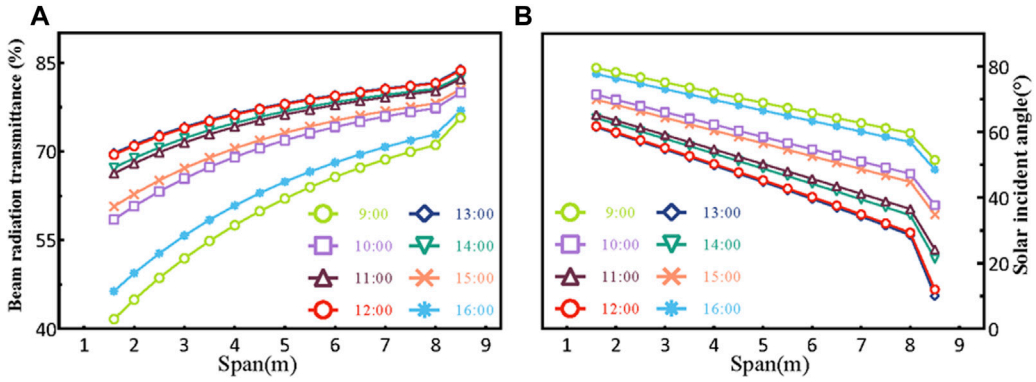

FIGURE 6
Diurnal variation in **(A)** the solar radiation incident angle and **(B)** transmittance of the roof.

radiation availability on the wall, and the measured values were accordingly underestimated.

3.2 Analysis of the light environment construction of the solar greenhouse

The calculated results of the fitted roof curve and slope angle were obtained using the model (Figure 5). The slope angle was different at different positions on the roof and increased from north to south. The north roof slope angle were −49.02° to −24.96°, and the south roof slope angle were 2.56°–80.35°. Thus, the incident angle of the beam solar radiation on the curved roof varied with the slope angle, affecting the transmitted beam solar radiation.

To maximize solar radiation obtained through a curved roof, based on the theory of a reasonable daylighting period (Li, 2014), the beam radiation incident angle must be less than 40° from 10:00 to 14:00 during the winter solstice. On a simulated sunny winter Solstice day, the incident angle varies with time of day and position on the roof (Figure 6). The incident angle variations were 51.5°–79.3°, 37.7°–71.4°, 24.2°–65.3°, 11.9°–61.8°, 10.1°–61.5°, 21.4°–64.3°, 34.82°–68.9°, and 48.5°–77.6° at 9:00, 10:00, 11:00, 12:00, 13:00, 14:00, 15:00, and 16:00, respectively. As previously stated, the theoretical incident angle in the range of 0°–40° on a simplified and equivalent inclined roof changes with time, whereas the actual incident angle changes with time and position on the curved roof. When taking the greenhouse roof as a tilting roof with an equivalent slope angle of 30°, the incident angle and average transmittance of the greenhouse were 38.9°–53.3° and 74.8%–80.6% from 10:00 to 14:00, whereas those of the curved roof were 43.3°–68.5° and 70.7%–77.9%, respectively. Thus, the transmitted beam radiation inside a greenhouse with an inclined roof may have been overestimated. Additionally, the dynamic and nonuniform radiation transmittance on the roof causes a spatial distribution difference in the transmitted radiation inside the greenhouse.

The spatial distribution of the transmitted solar radiation can describe the light environment of a solar greenhouse, which directly and dynamically influences light demand and utilization for crop production and effectively improves the additional need for heat energy supply. Following the model established above, the dynamic spatial distribution of solar radiation inside a greenhouse can be simulated accurately and efficiently. The CSG-ITB has its simulated spatial distribution of the average radiation intensity on a hypothetical and typical sunny day during the winter solstice, which can objectively reflect the basic daily light performance inside a greenhouse because it has the shortest daytime during the winter (Figure 7). The radiation distribution exhibited significant spatial differences that change along the span from south to north (Figure 7). As previously mentioned, the roof slope angle influenced the incident angle of beam radiation, consequently altering the transmittances of the roof. Consequently, a greater amount of solar radiation was transmitted into the southern part of the solar greenhouse compared to the northern part. Furthermore, due to variations in transmittance levels creating a complex light environment within the solar greenhouse, crop utilization of solar radiation was affected. Therefore, it is imperative to verify the spatial distribution of solar radiation within a solar greenhouse to ensure that the light environment provided meets the requirements for crop.

Due to the transparent north roof and internal thermal blanket, the entire roof was fully transparent, allowing for enhanced solar radiation penetration. Although the solar radiation intensity was lower in the northern region of the CSG-ITB, no shadow region was observed due to the presence of an opaque north roof and an external thermal blanket, which are characteristic features of a typical CSG. Taking the horizontal plane of the crop canopy height (1.5 m) as an example, the radiation intensity gradually decreased from the south roof to the north wall in the range of 178.5–210.6 W/m^2. The difference in radiation intensity from south to north in terms of crop canopy height without planting crops was small; however, the radiation intensity variation may increase with crop growth.

Because energy-saving solar greenhouses operate without auxiliary heating, solar energy is the only energy required to meet plant and greenhouse energy requirements. Captured, transmitted, and stored solar energy are crucial for maintaining the greenhouse energy balance. The north wall is an important greenhouse section that absorbs solar energy. Figure 8 shows the solar radiation accumulation captured and transmitted by the greenhouse roof and its allocation to the interior surfaces of the

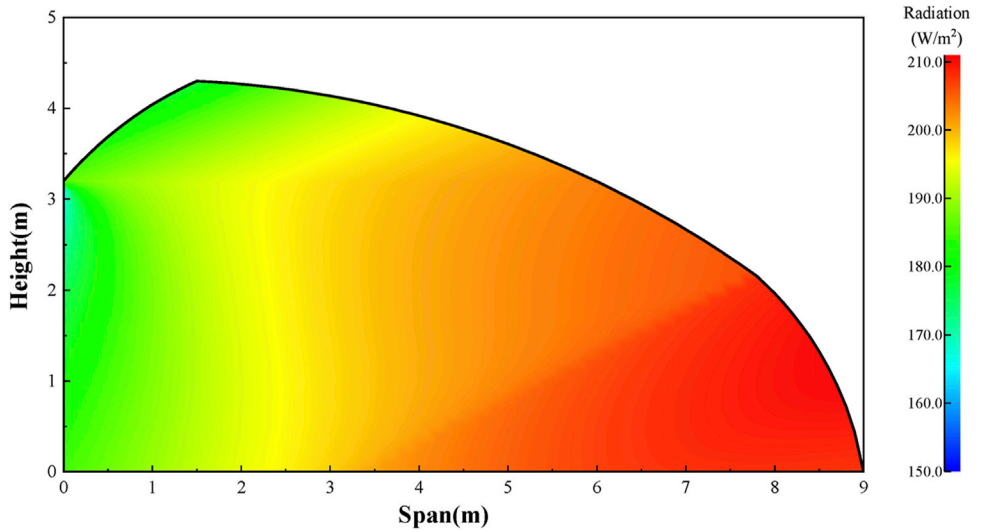

FIGURE 7
Diurnal spatial distribution of the average solar radiation intensity on a clear and sunny day on the winter solstice for the solar greenhouse with an internal thermal blanket.

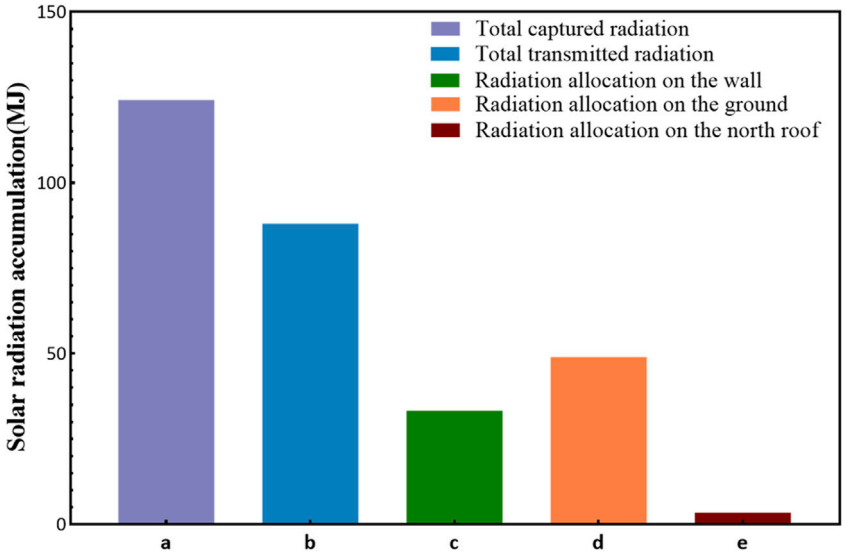

FIGURE 8
Diurnal solar radiation accumulation on different surfaces of the solar greenhouse interior: **(A)** total captured solar radiation; **(B)** total transmitted solar radiation; **(C)** solar radiation allocation on the wall; **(D)** solar radiation allocation on the ground; and **(E)** solar radiation allocation on the north roof.

greenhouse. The calculated accumulations of the captured and transmitted radiation were 124.2 and 87.99 MJ, respectively, indicating that 70.85% of the solar energy enters the greenhouse through the roof from 9:00 to 16:00 and projects on the greenhouse surfaces. The wall, ground, and north roof (although transparent) received part of the transmitted radiation, and the cumulative values were 33.25, 48.96, and 3.41 MJ, respectively. The allocation on the wall and ground were 37.79% and 55.64%, respectively. However, the wall was approximately 1/3 of the ground area. Thus, the wall stores energy more efficiently than the ground, which should be enhanced by increasing the wall height within a reasonable and economical range.

3.3 Influence of solar radiation of solar greenhouses with different roof structures

The correlation among structural parameters must be considered when designing a solar greenhouse. The span length and ridge height determine the size of a solar greenhouse, whereas the north wall height, north roof length and slope angle, and equivalent slope of the south roof

TABLE 1 Structure parameters of simulated solar greenhouses.

	Coverage type	Roof type	Equivalent roof angle (°)	Length(m)	Span(m)	Wall height(m)	Ridge height(m)
SG1	Internal Coverage	Curved	30.0	50.0	9.0	3.2	4.3
SG2	External Coverage	Curved	30.0	50.0	9.0	3.2	4.3
SG3	External Coverage	Inclined	30.0	50.0	9.0	3.2	4.3

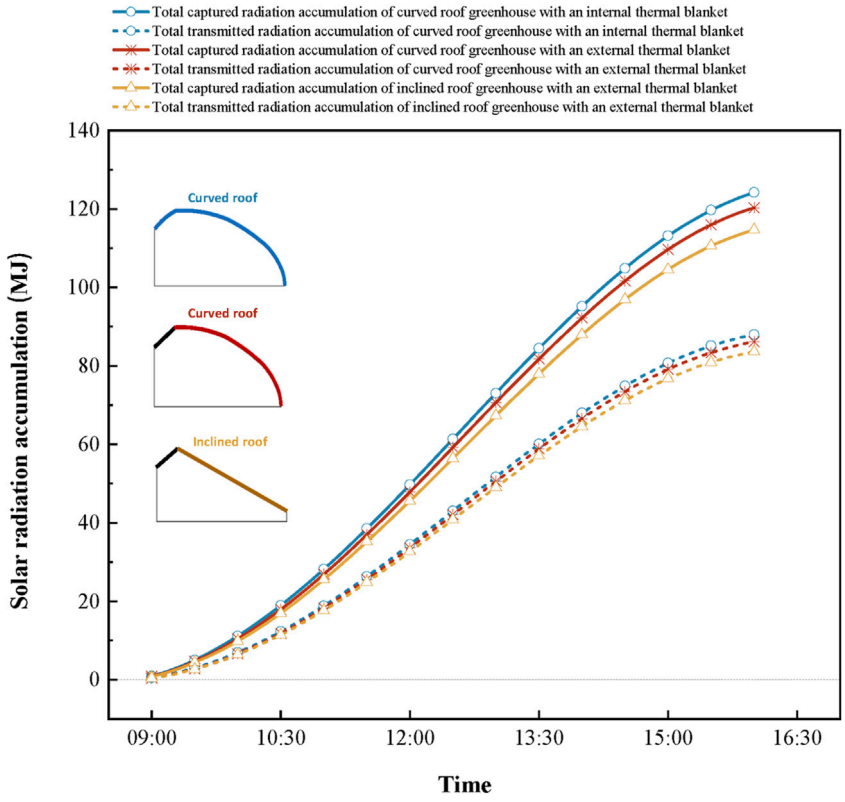

FIGURE 9
Diurnal captured and transmitted solar radiation accumulation of solar greenhouses with different roof shapes.

affect the shape of the greenhouse under fixed span length and ridge height conditions. In other words, greenhouses of the same size differ, including in terms of their radiation performances. In order to assess the disparity in light performance among different roof structures of greenhouse, three solar greenhouses with distinct roof shapes were conducted simulations. The specifications of these simulated solar greenhouses are presented in Table 1.

Figure 9 presents the influence of the roof shape on the captured and transmitted radiation accumulation. The three objective greenhouses had the same size and different shapes. The curved-roof greenhouses achieved more captured and transmitted radiation accumulation than the inclined-roof greenhouse. The greenhouse with an internal thermal blanket absorbed the most radiation on a sunny day. Compared with the two other greenhouses with external blankets, the greenhouse featuring an internal blanket exhibited an increase in captured and transmitted radiation accumulation of 3.9 and 1.8 MJ compared to the curved-roof greenhouse, 9.5 and 4.4 MJ, respectively, over the inclined-roof greenhouse. This can be primarily attributed to the absence of an opaque north roof and external blanket shading, which facilitated a higher capture of diffuse radiation. Furthermore, under conditions where an external thermal blanket cover was present, the opaque north roof retained heat in typical solar greenhouses that lack the ability to absorb and store solar energy but possess a north wall for enhancing thermal environment. However, for a greenhouse equipped with an internal thermal blanket, it appears that the role of the north roof in heat preservation is less significant. Therefore, there is a need to reconsider its function in solar greenhouse design theory in order to optimize its performance.

3.4 Effect of the position of the internal rolling thermal blanket on solar greenhouse light performance

A greenhouse receives solar radiation when a thermal blanket opens after sunrise and closes before sunset. The thermal blanket

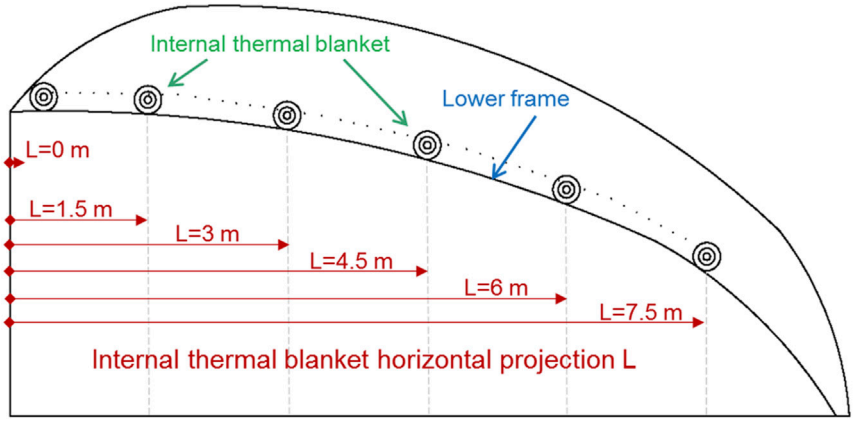

FIGURE 10
Schematic diagram of solar greenhouses with different lengths of blanket horizontal projection.

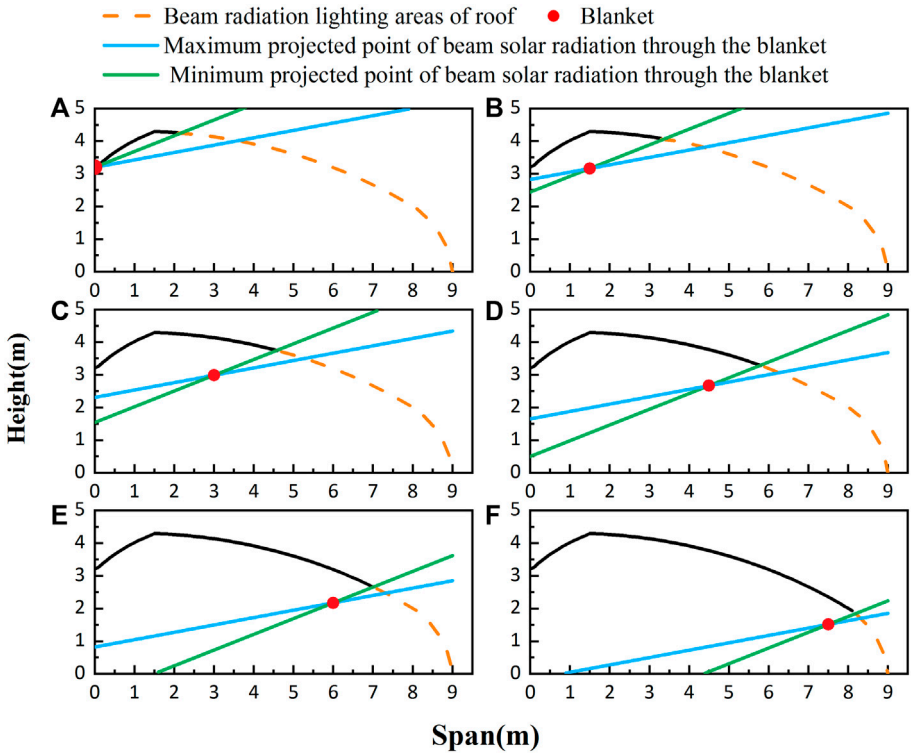

FIGURE 11
Projection position of beam solar radiation through the lower edge of the blanket with different blanket projection lengths: **(A)** L = 0 m; **(B)** L = 1.5 m; **(C)** L = 3 m; **(D)** L = 4.5 m; **(E)** L = 6 m; **(F)** L = 7.5 m.

covers the roof at night to reduce heat loss. However, the blanket may be positioned improperly on the roof, partially blocking the beam radiation projecting onto the wall and ground during the lighting period. The increasing shadow area on the wall caused by blanket shading reduces the solar energy obtained, negatively affecting the thermal environment inside the greenhouse. In theory, the best position is the highest point of the south roof, which is lit; however, this method is not available in practice for safety or other reasons. The blanket length covered on the roof can directly exhibit influence the greenhouse light environment at varying degrees. For a solar greenhouse with an external thermal blanket, the blanket can be installed at a sufficiently high height to optimize the lighting ability of the south roof. However, the position of the internal blanket was lower than that of the blanket in the upper and exterior frames in the vertical direction, and the influence of the shading on the wall was

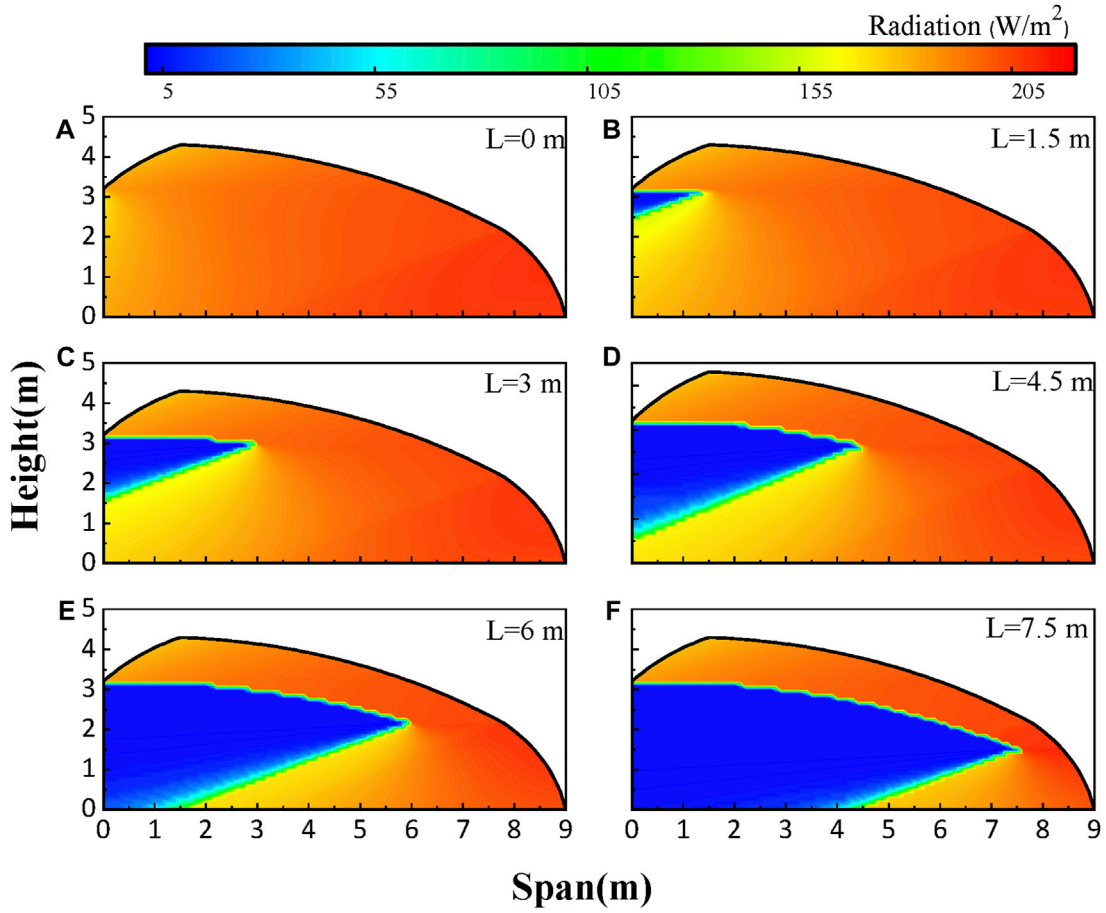

FIGURE 12
Diurnal spatial distribution of the average solar radiation intensity inside the greenhouse with different blanket projection lengths.

inevitably severe when the horizontal projection lengths were the same.

Figure 10 shows the different positions of the internal blanket in the lower frame of the greenhouse. Along the span direction from north to south, both the blanket-covered length and length of the horizontal projection increased. The beam solar radiation projected on the wall and ground varied with time and blanket-covered length (Figure 11). The projected point of beam radiation changed dynamically during the daytime, directly affecting the region receiving beam radiation. The area of the radiation projection was the largest when the sun was at low altitudes, and it was smaller when the sun was at high altitudes. The area variation increased with increasing blanket-covered length (Figures 11A–E), and the beam radiation did not project on the wall when the length of the horizontal projection of the blanket was 7.5 m (L = 7.5 m) (Figure 11F).

The blanket's position affected the transmitted radiation allocation on the surfaces on which the solar energy can be converted to heat for storage/release and worsened the spatial distribution of the solar radiation inside (Figure 12). The lighting demands of crops in the plant region under the blanket, varying with blanket-covered length (Figures 12A–F), were increasingly implacable, thereby severely limiting the normal growth of crops and significantly affecting the production efficiency of solar greenhouses. The calculated amount of radiation projected on the wall and ground revealed that radiation accumulation decreased with increasing blanket-covered length (Figure 13). Compared with the blanket-covered length of 0 m, the 1.5, 3, 4.5, 6, and 7.5 m lengths of horizontal projection (Figures 13A–F) decreased the cumulative radiation by 25.24%, 66.58%, 73.08%, 97.46%, and 99.82% on the wall and 1.60%, 3.49%, 5.69%, 18.06%, and 47.47% on the ground, respectively. Moreover, for every 0.1 m decrease in the average projection length of the beam radiation on the wall, the cumulative radiation decreased by approximately 1.04–1.31 MJ. The results demonstrate that the energy storage capacity of the wall decreases, and greenhouse energy consumption increases with increasing horizontal projection length. Therefore, the parking positions of the blankets must be reasonably controlled for greenhouse users to promote management efficiency and energy-saving production.

4 Conclusion

Achieving more efficient solar energy utilization is critical to sustainable solar greenhouse development. With the perfection of structural design theory and the practical application of novel heat

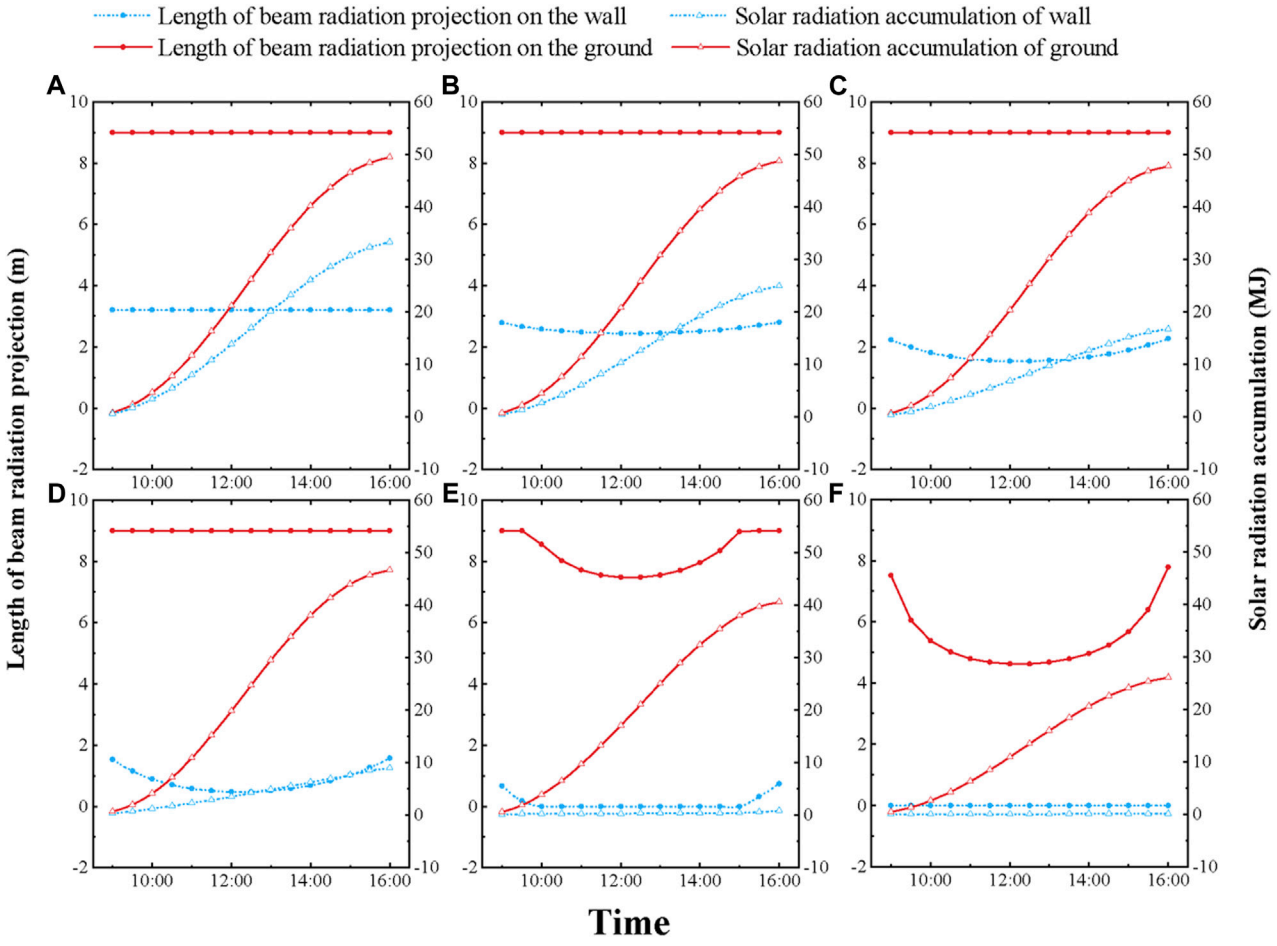

FIGURE 13
Dynamic variation in beam solar radiation projected points and solar radiation accumulation on the wall and ground inside the greenhouse.

management technology, the light and thermal performance of CSGs has been improved to suit different climate conditions for cultivation in all seasons. In this study, the light performance of a novel CSG with an internal thermal blanket was evaluated using a mathematical solar radiation model. By assuming the simulated day as a clear and sunny day on the winter solstice, the effects of the spatial relationship between the greenhouse and the sun, the spatial distribution in the greenhouse, and the position of the blanket on the light environment were investigated based on the simulated results of the model. The following conclusions were obtained:

(1) The reliability of the established model was verified by comparing the consistencies between the measured and simulated values.
(2) The spatial distribution of the transmitted solar radiation declined from south to north. These results are generally caused by the difference in the beam solar radiation transmittance along the curved roof from the bottom to the top. The solar radiation allocation on the wall was less than that on the ground; however, within the same area, the wall received more solar radiation than the ground. Thus, the wall's contribution to the solar energy collection was non-negligible.
(3) Under limited-size conditions, the shape of the greenhouse roof influenced the accumulation of captured and transmitted radiation. The curved-roof greenhouses accumulated more solar radiation than the inclined-roof greenhouse. Moreover, the greenhouse with an internal blanket received more diffuse radiation because its roof was entirely transparent.
(4) The solar energy received on the wall was significantly affected by the horizontal projection length of the north roof and blanket horizontal projection length. This is disadvantageous in a solar greenhouse with an internal thermal blanket. Varying with blanket horizontal projection length, the cumulative radiation on the wall decreased by 25.24%–99.82%, indicating that for every 0.1 m decrease in the average projection length of the beam solar radiation on the wall, the cumulative radiation decreased by approximately 1.04–1.31 MJ.

The established model was validated as an accurate method for analyzing the light performance of a solar greenhouse and can be adapted to all types of greenhouses. In addition, because of the complex conditions on cloudy days, solar radiation on cloudy days was not considered. Long-term variations in solar radiation inside greenhouses must be investigated in the future.

Data availability statement

The original contributions presented in the study are included in the article/Supplementary Material, further inquiries can be directed to the corresponding author.

Author contributions

SC conceptualized and designed the study. QS handled the software. YS and SC performed and supervised the experiments. YS and ZY performed the formal analysis. QS, ZY, and XL performed the investigation, and QS, ZY, and XL validated the results. QS, YS, and SC wrote, reviewed, and edited the manuscript. All authors contributed to the article and approved the submitted version.

Funding

This work was supported by the National Natural Science Foundation of China (31860573), National Key Research and Development Program of China (SQ2023YFD2000083), Inner Mongolia Scientific and Technological Achievements Transformation Project (CGZH2018039) and the Key Project of Science and Technology for the Development of Inner Mongolia (KJXM-EEDS-2020008).

Conflict of interest

The authors declare that the research was conducted in the absence of any commercial or financial relationships that could be construed as a potential conflict of interest.

Publisher's note

All claims expressed in this article are solely those of the authors and do not necessarily represent those of their affiliated organizations, or those of the publisher, the editors and the reviewers. Any product that may be evaluated in this article, or claim that may be made by its manufacturer, is not guaranteed or endorsed by the publisher.

References

Aldaftari, H. A., Okajima, J., Komiya, A., and Maruyama, S. (2019). Radiative control through greenhouse covering materials using pigmented coatings. *J. Quant. Spectrosc. Radiat. Transf.* 231, 29–36. doi:10.1016/j.jqsrt.2019.04.009

Bazgaou, A., Fatnassi, H., Bouharroud, R., Elame, F., Ezzaeri, K., Gourdo, L., et al. (2020a). Performance assessment of combining rock-bed thermal energy storage and water filled passive solar sleeves for heating Canarian greenhouse. *Sol. Energy* 198, 8–24. doi:10.1016/j.solener.2020.01.041

Bazgaou, A., Fatnassi, H., Bouharroud, R., Ezzaeri, K., Gourdo, L., Wifaya, A., et al. (2020b). Effect of active solar heating system on microclimate, development, yield and fruit quality in greenhouse tomato production. *Renew. Energy* 165 (2021), 237–250. doi:10.1016/j.renene.2020.11.007

Bibbiani, C., Campiotti, C. A., Schettini, E., and Vox, G. (2017). A sustainable energy for greenhouses heating in Italy: wood biomass. *Acta Hortic.* (1170), 523–530. doi:10.17660/ActaHortic.2017.1170.65

Bot, G., Van De Braak, N., Challa, H., Hemming, S., Rieswijk, T., van Straten, G., et al. (2005). The solar greenhouse: state of the art in energy saving and sustainable energy supply. *Acta Hortic.* 691 (2), 501–508. doi:10.17660/ActaHortic.2005.691.59

Çakır, U., and Şahin, E. (2015). Using solar greenhouses in cold climates and evaluating optimum type according to sizing, position and location: a case study. *Comput. Electron. Agric.* 117, 245–257. doi:10.1016/j.compag.2015.08.005

Canakci, M., Emekli, N. Y., Bilgin, S., and Caglayan, N. (2013). Heating requirement and its costs in greenhouse structures: a case study for Mediterranean region of Turkey. *Renew. Sustain. Energy Rev.* 24, 483–490. doi:10.1016/j.rser.2013.03.026

Chen, C., Li, Y., Li, N., Wei, S., Yang, F., Ling, H., et al. (2018). A computational model to determine the optimal orientation for solar greenhouses located at different latitudes in China. *Sol. Energy* 165, 19–26. doi:10.1016/j.solener.2018.02.022

Chen, X., Shuai, C., Zhang, Y., and Wu, Y. (2020). Decomposition of energy consumption and its decoupling with economic growth in the global agricultural industry. *Environ. Impact Assess. Rev.* 81, 106364. doi:10.1016/j.eiar.2019.106364

Cossu, M., Murgia, L., Ledda, L., Deligios, P. A., Sirigu, A., Chessa, F., et al. (2014). Solar radiation distribution inside a greenhouse with south-oriented photovoltaic roofs and effects on crop productivity. *Appl. Energy* 133, 89–100. doi:10.1016/j.apenergy.2014.07.070

Cuce, E., Harjunowibowo, D., and Cuce, P. M. (2016). Renewable and sustainable energy saving strategies for greenhouse systems: a comprehensive review. *Renew. Sustain. Energy Rev.* 64, 34–59. doi:10.1016/j.rser.2016.05.077

El-Maghlany, W. M., Teamah, M. A., and Tanaka, H. (2015). Optimum design and orientation of the greenhouses for maximum capture of solar energy in North Tropical Region. *Energy Convers. manage.* 105, 1096–1104. doi:10.1016/j.enconman.2015.08.066

Esmaeli, H., and Roshandel, R. (2020). Optimal design for solar greenhouses based on climate conditions. *Renew. Energy* 145, 1255–1265. doi:10.1016/j.renene.2019.06.090

Gorjian, S., Calise, F., Kant, K., Ahamed, M. S., Copertaro, B., Najafi, G., et al. (2021). A review on opportunities for implementation of solar energy technologies in agricultural greenhouses. *J. Clean. Prod.* 285, 124807. doi:10.1016/j.jclepro.2020.124807

Han, Y., Xue, X., Luo, X., Guo, L., and Li, T. (2014). Establishment of estimation model of solar radiation within solar greenhouse. *Trans. Chin. Soci. Agric. Eng.* 30 (10), 174–181. doi:10.3969/j.issn.1002-6819.2014.10.022

Hassanien, R. H. E., Li, M., and Lin, W. D. (2016). Advanced applications of solar energy in agricultural greenhouses. *Renew. Sustain. Energy Rev.* 54, 989–1001. doi:10.1016/j.rser.2015.10.095

Huang, L., Deng, L., Li, A., Gao, R., Zhang, L., and Lei, W. (2020). Analytical model for solar radiation transmitting the curved transparent surface of solar greenhouse. *J. Build. Eng.* 32, 101785. doi:10.1016/j.jobe.2020.101785

Li, J., Bai, Q., and Zhang, Y. (2010). Analysis on measurement of heat absorption and release of wall and ground in solar greenhouse. *Trans. Chin. Soci. Agric. Eng.* 26 (4), 231–236. doi:10.3969/j.issn.1002-6819.2010.04.039

Li, T. (2014). *Theory and practice on vegetable cultivation in solar greenhouse*. Beijing: China Agricultural Press.

Liu, X., Wu, X., Xia, T., Fan, Z., Shi, W., Li, Y., et al. (2022). New insights of designing thermal insulation and heat storage of Chinese solar greenhouse in high latitudes and cold regions. *Energy* 242, 122953. doi:10.1016/j.energy.2021.122953

Lund, J. W., Freeston, D. H., and Boyd, T. L. (2005). Direct application of geothermal energy: 2005 Worldwide review. *Geothermics* 34 (6), 691–727. doi:10.1016/j.geothermics.2005.09.003

Ma, C., Zhao, S., Cheng, J., Wang, N., Jiang, Y., Wang, S., et al. (2013). On establishing light environment model in Chinese solar greenhouse. *J. Shengyang. Agric. Univ.* 44 (5), 513–517. doi:10.3969/j.issn.1000-1700.2013.05.001

Raptis, P., Kazadzis, S., Psiloglou, B., et al. (2017). Measurements and model simulations of solar radiation at tilted planes, towards the maximization of energy capture. *Energy* 130, 570–580. doi:10.1016/j.energy.2017.04.122

Sethi, V. P. (2009). On the selection of shape and orientation of a greenhouse: thermal modeling and experimental validation. *Sol. Energy* 83 (1), 21–38. doi:10.1016/j.solener.2008.05.018

Shukla, A., Sharma, A., and Kant, K. (2016). Solar greenhouse with thermal energy storage: a review. *Curr. Sustain.Renew.Energy Rep.* 3 (3-4), 58–66. doi:10.1007/s40518-016-0056-y

Singh, R., and Tiwari, G. (2010). Energy conservation in the greenhouse system: a steady state analysis. *Energy* 35 (6), 2367–2373. doi:10.1016/j.energy.2010.02.003

Taki, M., Rohani, A., and Rahmati-Joneidabad, M. (2018). Solar thermal simulation and applications in greenhouse. *Inf. Process. Agric.* 5 (1), 83–113. doi:10.1016/j.inpa.2017.10.003

Tang, Y., Ma, X., Li, M., and Wang, Y. (2020). The effect of temperature and light on strawberry production in a solar greenhouse. *Sol. Energy* 195, 318–328. doi:10.1016/j.solener.2019.11.070

Tong, G., Christopher, D. M., Li, T., and Bai, Y. (2010). Influence of thermal blanket position on solar greenhouse temperature distributions. *Trans. Chin. Soci. Agric. Eng.* 26 (10), 253–258. doi:10.3969/j.issn.1002-6819.2010.10.043

Tong, G., Chen, Q., and Xu, H. (2022). Passive solar energy utilization: a review of envelope material selection for Chinese solar greenhouses. *Sustain. Energy Technol. Assess.* 50, 101833. doi:10.1016/j.seta.2021.101833

Tong, G., Christopher, D. M., and Zhang, G. (2018). New insights on span selection for Chinese solar greenhouses using CFD analyses. *Comput. Electron. Agric.* 149, 3–15. doi:10.1016/j.compag.2017.09.031

Tong, G., and Li, B. (2006). Simulation of solar radiation on surfaces of a solar greenhouse. *J. Chin. Agric. Univ.* 11 (1), 61–65. doi:10.3321/j.issn:1007-4333.2006.01.013

Trypanagnostopoulos, G., Kavga, A., Souliotis, M., and Tripanagnostopoulos, Y. (2017). Greenhouse performance results for roof installed photovoltaics. *Renew. Energy* 111, 724–731. doi:10.1016/j.renene.2017.04.066

Vadiee, A., and Martin, V. (2012). Energy management in horticultural applications through the closed greenhouse concept, state of the art. *Renew. Sustain. Energy Rev.* 16 (7), 5087–5100. doi:10.1016/j.rser.2012.04.022

Wang, C., Shi, W., Pei, X., Yuan, S. C., Kuo, P. C., Chuang, H. L., et al. (2010). Cigarette smoking and cognitive impairment: a 10-year cohort study in Taiwan. *J.Northwest A F Univ.* 38 (8), 143–148. doi:10.1016/j.archger.2009.09.041

Wei, B., Guo, S., Wang, J., Li, J., Wang, J., Zhang, J., et al. (2016). Thermal performance of single span greenhouses with removable back walls. *Biosyst. Eng.* 141, 48–57. doi:10.1016/j.biosystemseng.2015.11.008

Wu, R., Wu, R., Jin, L., Wang, H. Z., Liu, S. N., Jiang, S. J., et al. (2023). Climate suitability division of solar greenhouse in Inner Mongolia Autonomous Region, China. *Chin. J. Appli. Ecol.* 34 (5), 1305–1312. doi:10.13287/j.1001-9332.202305.027

Xu, D., Li, Y., Zhang, Y., Xu, H., Li, T., and Liu, X. (2020). Effects of orientation and structure on solar radiation interception in Chinese solar greenhouse. *PLoS One* 15 (11), e0242002. doi:10.1371/journal.pone.0242002

Xu, H., Cao, Y., Li, Y., Tan, B., and Wang, J. (2019). Effects of *Bacillus thuringiensis* genetic engineering on induced volatile organic compounds emission in maize and the attractiveness to a parasitic wasp. *Trans. Chin. Soci. Agric. Eng.* 35 (7), 160–169. doi:10.3389/fbioe.2019.00160

Zhang, X., Wang, H., Zou, Z., and Wang, S. (2016). CFD and weighted entropy based simulation and optimisation of Chinese Solar Greenhouse temperature distribution. *Biosyst. Eng.* 142, 12–26. doi:10.1016/j.biosystemseng.2015.11.006

Zhang, X., Lv, J., Xie, J., Yu, J., Zhang, J., Tang, C., et al. (2020). Solar radiation allocation and spatial distribution in Chinese solar greenhouses: model development and application. *Energies* 13 (5), 1108. doi:10.3390/en13051108

Zhang, Y., Zou, Z., and Li, J. (2014). Performance experiment on lighting and thermal storage in tilting roof solar-greenhouse. *Trans. Chin. Soci. Agric. Eng.* 30 (1), 129–137. doi:10.3969/j.issn.1002-6819.2014.01.017

Nomenclature

A	solar azimuth angle (°)
a	greenhouse azimuth angle (°)
DN	days number
ET	the time difference between the local position and Beijing
h	solar altitude angle (°)
I_0	solar radiation constant (W/m^2)
I_b, I_d	solar beam and diffuse radiation (W/m^2)
L	the length of the greenhouse component (m)
M	the mass of the atmosphere
P	a point
P	atmosphere transparency coefficient
Q	the solar radiation accumulation (MJ)
S	the length of the connection line between roof and projected surface (m)
T_{LOCAL}, $T_{STANDARD}$	the local apparent solar time and the Beijing time
X	the view factor from roof to projected surface
Greek letters	
β	the slope angle of the roof (°)
γ_{LOCAL}, $\gamma_{STANDARD}$	the local longitude and standard longitude of Beijing time (°)
δ	the solar declination angle (°)
ε	the angle between the connection line and its normal (°)
θ	the incident angle of the beam solar radiation (°)
σ_1, σ_2, σ_3	the solar radiation transmission attenuation
τ_b	the solar beam radiation transmittance
τ_{b0}	the beam radiation transmittance of a clear transparent film at an incident angle of 0°
τ_d	the solar diffuse radiation transmittance
τ_{d0}	the diffuse radiation transmittance of a clear transparent film
ϕ_{LOCAL}	the geographical latitude of solar greenhouse (°)
ω	the hour angle (°)
Subscripts and Superscripts	
cap	captured
cl	the closing time of the blanket
op	the opening time of the blanket
g	ground
ic	incident
pj	projected
RH	ridge height
roof	greenhouse roof
SP, span	greenhouse span
ss	the time of sunset
sr	the time of sunrise
t	time
trans	transmitted
WH	wall height